

# Chemical Beam Deposition of MgO Films on Si Substrates Using Methylmagnesium *tert*-Butoxide

Myung M. Sung,<sup>†</sup> Chang G. Kim,<sup>‡</sup> Jinkwon Kim,<sup>§</sup> and Yunsoo Kim<sup>\*,‡</sup>

*Thin Film Materials Laboratory, Advanced Materials Division, Korea Research Institute of Chemical Technology, Yuseong P.O. Box 107, Daejeon 305-600, South Korea, Department of Chemistry, Kookmin University, Seoul 136-702, South Korea, and Department of Chemistry and RRC/NMR, Kongju National University, Kongju 314-701, South Korea*

Received July 25, 2001. Revised Manuscript Received October 18, 2001

MgO films have been grown on Si(111) and Si(100) substrates at 400–800 °C by using methylmagnesium *tert*-butoxide as a single precursor under high-vacuum conditions ( $5 \times 10^{-6}$  Torr). The methylmagnesium *tert*-butoxide precursor was synthesized and characterized by spectroscopic methods and single-crystal X-ray diffraction analysis. The chemical composition, crystalline structure, and morphology of the deposited films were investigated by X-ray photoelectron spectroscopy, X-ray diffraction, X-ray pole figure analysis, and scanning electron microscopy. The results show that epitaxial MgO films with correct stoichiometry can be deposited on Si(111) at 800 °C, whereas highly [100] oriented MgO films are deposited on Si(100) at 800 °C. Thermal desorption studies indicate that the precursor is decomposed into isobutene and methane via  $\beta$ -hydrogen elimination. The single precursor methylmagnesium *tert*-butoxide has been found suitable for chemical beam deposition of MgO thin films on Si substrates.

## Introduction

Magnesium oxide is thermodynamically very stable, has a low dielectric constant and a low refractive index, and has been widely used as substrate for growing various thin-film materials. The oxygen lattice of MgO crystal matches well with those of perovskite oxide crystals and those of Si and GaAs crystals. MgO buffer layers were used to grow high  $T_c$  superconductors<sup>1,2</sup> and ferroelectrics<sup>3,4</sup> as well as a nitride.<sup>5</sup> Superconducting YBa<sub>2</sub>Cu<sub>3</sub>O<sub>7-x</sub> films were deposited epitaxially on MgO/GaAs(100) where MgO thin films were prepared by laser deposition or electron beam evaporation.<sup>6–8</sup> Also, ferroelectric LiNbO<sub>3</sub> films were epitaxially grown on MgO-(111)<sup>9</sup> because of the excellent match of the MgO(111) atomic spacings with those in the *a*–*b* planes of LiNbO<sub>3</sub>.

Several reports have been published on chemical vapor deposition (CVD) of MgO, although MgO films

were more frequently prepared by physical vapor deposition methods such as electron beam evaporation, pulsed laser deposition, and sputter deposition. Various magnesium compounds have been used as CVD sources. These are diethylmagnesium,<sup>10</sup> bis(2,2,6,6-tetramethyl-3,5-heptanedionato)magnesium,<sup>11–14</sup> bis(acetylacetonato)magnesium,<sup>15–17</sup> magnesium acetate,<sup>18</sup> magnesium 2-ethylhexanoate,<sup>19</sup> and bis(cyclopentadienyl)magnesium.<sup>20</sup> These compounds must be vaporized at high temperatures (higher than 100 °C except in diethylmagnesium) and generally need an additional oxygen source such as H<sub>2</sub>O and O<sub>2</sub>. More recent studies with newly synthesized precursors such as a magnesium  $\beta$ -diketonatoalkoxide,<sup>21</sup> a magnesium  $\beta$ -ketoiminate,<sup>22</sup> and a polydentate amine complex of a magnesium  $\beta$ -diketonate<sup>23</sup> yielded good results regarding vaporiza-

\* To whom all correspondence should be addressed. E-mail: yunsukim@kricr.re.kr.

<sup>†</sup> Kookmin University.

<sup>‡</sup> Korea Research Institute of Chemical Technology.

<sup>§</sup> Kongju National University.

(1) Wang, F.; Müller, S.; Wördenweber, R. *Thin Solid Films* **1993**, *232*, 232.

(2) Tseng, M. Z.; Jiang, W. N.; Hu, E. L. *J. Appl. Phys.* **1994**, *76*, 3562.

(3) Hsu, W.-Y.; Raj, R. *Appl. Phys. Lett.* **1992**, *60*, 3105.

(4) Fork, D. K.; Anderson, G. B. *Appl. Phys. Lett.* **1993**, *63*, 1029.

(5) Tonouchi, M.; Sakaguchi, Y.; Kobayashi, T. *J. Appl. Phys.* **1987**, *62*, 961.

(6) Fork, D. K.; Nashimoto, K.; Geballe, T. H. *Appl. Phys. Lett.* **1992**, *60*, 1621.

(7) Chang, L. D.; Tseng, M. Z.; Hu, E. L.; Fork, D. K. *Appl. Phys. Lett.* **1992**, *60*, 1753.

(8) Prusseit, W.; Corsépius, S.; Baudenbacher, F.; Hirata, K.; Berberich, P.; Kinder, H. *Appl. Phys. Lett.* **1992**, *61*, 1841.

(9) Matsunaga, H.; Ohno, H.; Okamoto, Y.; Nakajima, Y. *J. Cryst. Growth* **1990**, *99*, 630.

(10) Huang, R.; Kitai, A. H. *Appl. Phys. Lett.* **1992**, *61*, 1450.

(11) Kwak, B. S.; Boyd, E. P.; Zhang, K.; Erbil, A.; Wilkins, B. *Appl. Phys. Lett.* **1989**, *54*, 2542.

(12) Zhao, Y.-W.; Suhr, H. *Appl. Phys. A* **1992**, *54*, 451.

(13) Lu, Z.; Feigelson, R. S.; Route, R. K.; DiCarolis, S. A.; Hiskes, R.; Jacowitz, R. D. *J. Cryst. Growth* **1993**, *128*, 788.

(14) Boo, J.-H.; Yu, K.-S.; Koh, W.; Kim, Y. *Mater. Lett.* **1996**, *26*, 233.

(15) Kamata, K.; Shibata, Y.; Kishi, Y. *J. Mater. Sci. Lett.* **1984**, *3*, 423.

(16) Fujii, E.; Tomozawa, A.; Fujii, S.; Torii, H.; Hattori, M.; Takayama, R. *Jpn. J. Appl. Phys.* **1993**, *32*, L1448.

(17) Fujii, E.; Tomozawa, A.; Fujii, S.; Torii, H.; Hattori, M.; Takayama, R. *Jpn. J. Appl. Phys.* **1994**, *33*, 6331.

(18) Vallet-Regi, M.; Labeau, M.; García, E.; Cabañas, M. V.; González-Calbet, J. M.; Delabouglise, G. *Physica C* **1991**, *180*, 57.

(19) Maruyama, T.; Shionoya, J. *Jpn. J. Appl. Phys.* **1990**, *29*, L810.

(20) Musolf, J.; Boeke, E.; Waffenschmidt, E.; He, X.; Heuken, M.; Heime, K. *J. Alloys Comp.* **1993**, *195*, 295.

(21) Davies, H. O.; Jones, A. C.; Leedham, T. J.; Crosbie, M. J.; Wright, P. J.; Boag, N. M.; Thompson, J. R. *Chem. Vap. Deposition* **2000**, *6*, 71.

(22) Matthews, J. S.; Just, O.; Obi-Johnson, B.; Rees, Jr., W. S. *Chem. Vap. Deposition* **2000**, *6*, 129.

tion characteristics, carbon incorporation, and crystallinity of the films deposited from them.

Using a single CVD source provides a novel alternative to conventional CVD that uses separate sources for the constituent elements of compound materials.<sup>24–27</sup> Gas-phase mixing is not necessary, and undesirable gas-phase reactions that can generate particles or impurity sources are much less likely to occur. Deposition usually proceeds at lower temperatures than conventional CVD. Methylmagnesium alkoxides and methylzinc alkoxides were known to produce MgO and ZnO, respectively, upon thermal decomposition.<sup>28</sup> Methylzinc alkoxides were successfully used to prepare ZnO films at 250 °C.<sup>29</sup>

In the present study, we have tried to grow MgO thin films epitaxially on Si substrates with only methylmagnesium *tert*-butoxide (MMTB)<sup>28,30–32</sup> as the single precursor. We found it to be a better source than conventional CVD sources for magnesium oxide (such as magnesium  $\beta$ -diketonates) previously reported in that the precursor, without any extra oxygen source, does not cause carbon incorporation into the growing MgO films because of its  $\beta$ -hydrogen elimination mechanism.

## Experimental Section

**Precursor Synthesis and Characterization.** All manipulations were performed under inert atmospheric conditions by using a glovebox or standard Schlenk techniques. All chemicals were purchased from Aldrich Chemical Co. The solvents were distilled from sodium/benzophenone and degassed before use. MMTB was synthesized from methylmagnesium bromide and potassium *tert*-butoxide. Methylmagnesium bromide (1.4 M in a 3:1 mixture of toluene and tetrahydrofuran) was used as received. Potassium *tert*-butoxide was recrystallized by sublimation. The <sup>1</sup>H and <sup>13</sup>C NMR spectra were recorded on a Bruker DPX 300 MHz spectrometer with chemical shifts referenced internally to benzene-*d*<sub>6</sub>.

Potassium *tert*-butoxide was slowly added to a solution of methylmagnesium bromide in a mixed solvent (toluene/tetrahydrofuran, 5:1) at 0 °C. The solution mixture was refluxed for 6 h. After filtering KBr, the solvent was removed under reduced pressure. The crude product was redissolved in hexane or toluene and extra KBr was filtered off. Then, the product was recrystallized by sublimation at 140 °C in vacuo. Colorless crystals were cropped from a supersaturated hexane solution at –40 °C. Yield: 93%. <sup>1</sup>H NMR (300.13 MHz, C<sub>6</sub>D<sub>6</sub>):  $\delta$  –0.70 (s, 3H, MgCH<sub>3</sub>), 1.35 [s, 9H, –OC(CH<sub>3</sub>)<sub>3</sub>]. <sup>13</sup>C {<sup>1</sup>H} NMR (75.47 MHz, C<sub>6</sub>D<sub>6</sub>):  $\delta$  –11.44, 32.37, 72.59.

A colorless crystal was mounted on a thin sealed glass capillary tube for X-ray crystallographic analysis. Intensity data were collected on an Enraf-Nonius CAD4 diffractometer equipped with monochromated Mo K $\alpha$  ( $\lambda$  = 0.71073 Å) radiation. Unit cell parameters were determined from a least-squares fit of 25 accurately centered reflections (19.44° < 2 $\theta$  < 31.17°). These dimensions and other parameters, including

**Table 1. Crystallographic Data for [Mg<sub>4</sub>Me<sub>4</sub>(O<sup>t</sup>Bu)<sub>4</sub>]**

temperature, °C	20
formula	C <sub>20</sub> H <sub>48</sub> Mg <sub>4</sub> O <sub>4</sub>
formular weight, g mol <sup>–1</sup>	449.82
space group	<i>P</i> $\bar{1}$
<i>a</i> , Å	9.680(2)
<i>b</i> , Å	17.937(3)
<i>c</i> , Å	28.031(5)
$\alpha$ , °	96.62(2)
$\beta$ , °	99.96(2)
$\gamma$ , °	105.68(1)
<i>V</i> , Å <sup>3</sup>	4547(2)
<i>Z</i>	6
$\rho$ (calcd), g cm <sup>–3</sup>	0.986
$\mu$ , mm <sup>–1</sup>	0.139
no. of unique reflections	12638
no. of observed reflections	7615 ( $F_o > 4\sigma(F_o)$ )
2 $\theta_{\max}$ , °	46
no. of variables	757
<i>R</i> ( <i>F</i> ), <i>wR</i> ( <i>F</i> <sup>2</sup> ), <sup>a</sup> GOF	0.0674, 0.1383, 1.190

<sup>a</sup>  $\omega = 1/[\sigma^2(F_o^2) + (0.056P)^2 + 2.5843P]$  where  $P = (F_o^2 + 2F_c^2)/3$ .

conditions of data collection, are summarized in Table 1. Data were collected at 20 °C in the  $\omega/2\theta$  scan mode. Three intense reflections were monitored every 200 reflections to check stability. Of the 12 638 unique reflections measured, 7615 were considered observed [ $F_o > 4\sigma(F_o)$ ] and were used in subsequent structure analysis. Data were corrected for Lorentz and polarization effects. Empirical  $\Psi$  absorption correction was applied. Maximum and minimum transmissions were 99.90% and 97.30%, respectively. The SHELXS-86 program was used for the direct method. The structure refinements were performed with the SHELXL-93 program on *F*<sup>2</sup> data. Anisotropic thermal parameters for all nonhydrogen atoms were included in the refinements. All hydrogen atoms bonded to carbon atoms were included in calculated positions. This C–H bond distance was fixed and *U* values were assigned based approximately on the *U* value of the attached atom. A final difference Fourier map revealed several random features (<0.21 eÅ<sup>–3</sup>).

**Chemical Beam Deposition and Characterization of MgO Thin Films.** A stainless steel ultrahigh vacuum (UHV) chamber was used for the growth of MgO thin films. The reactor was pumped by ion and turbomolecular pump combination achieving a base pressure lower than 1.0 × 10<sup>–9</sup> Torr. The gas line was pumped by an independent turbomolecular pump. The Si substrates used for the film growth in this research were cut from n-type (111) and (100) wafers with resistivity in the range 1–5 Ωcm. The Si substrates were initially treated by a chemical cleaning process, which involves degreasing, HNO<sub>3</sub> boiling, NH<sub>4</sub>OH boiling (alkali treatment), HCl boiling (acid treatment), rinsing in deionized water, and blow-drying with nitrogen, proposed by Ishizaka and Shiraki<sup>33</sup> to remove contaminants and grow a thin protective oxide layer on the surface. The substrates were introduced into the UHV chamber by means of a load-lock system. Substrate temperature was measured by an optical pyrometer through a 4.5-inch viewport in the chamber wall.

MMTB used as a single source for MgO in this work was transferred into a glass bulb attached to the gas-handling system under high-vacuum conditions (<1.0 × 10<sup>–8</sup> Torr) and was further purified by freeze–pump–thaw cycles with liquid nitrogen. The vapor of the precursor was introduced into the chamber through a variable leak valve (Granville-Phillips) and discharged from a nozzle located 3 cm above the substrate. The precursor bulb and the connecting stainless steel tubing were heated at ~140 °C.

Before the experiment, the chamber was pumped down to a pressure of low 10<sup>–9</sup> Torr, and then the substrate was mild-annealed at 650 °C for more than 5 h to minimize outgassing from the surface and the holder during deposition. Just before deposition, it was heated to 900 °C and annealed about 10 min

(23) Babcock, J. R.; Benson, D. D.; Wang, A.; Edleman, N. L.; Belot, J. A.; Metz, M. V.; Marks, T. J. *Chem. Vap. Deposition* **2000**, *6*, 180.

(24) Cowley, A. H.; Jones, R. A. *Angew. Chem., Int. Ed. Engl.* **1989**, *28*, 1208.

(25) Maury, F. *J. Phys. IV* **1995**, C5–449.

(26) Maury, F. *Chem. Vap. Deposition* **1996**, *2*, 113.

(27) Bochmann, M. *Chem. Vap. Deposition* **1996**, *2*, 85.

(28) Ashby, E. C.; Willard, G. F.; Goel, A. B. *J. Org. Chem.* **1979**, *44*, 1221.

(29) Auld, J.; Houlton, D. J.; Jones, A. C.; Rushworth, S. A.; Malik, M. A.; O'Brien, P.; Critchlow, G. W. *J. Mater. Chem.* **1994**, *4*, 1249.

(30) Coates, G. E.; Heslop, J. A.; Redwood, M. E.; Ridley, D. J. *J. Chem. Soc. A* **1968**, 1118.

(31) Ashby, E. C.; Nackashi, J.; Parris, G. E. *J. Am. Chem. Soc.* **1975**, *97*, 3162.

(32) Koh, W.; Ku, S.-J.; Kim, Y. *Bull. Korean Chem. Soc.* **1998**, *19*, 281.

(33) Ishizaka, A.; Shiraki, Y. *J. Electrochem. Soc.* **1986**, *133*, 666.

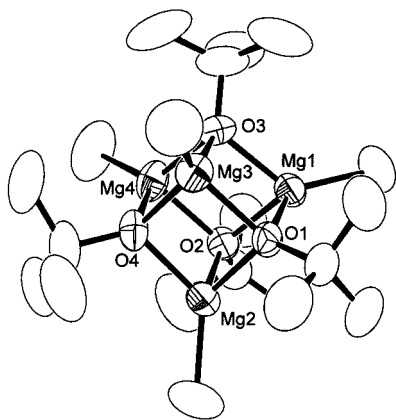


**Figure 1.** An ORTEP drawing of MMTB in tetrameric form.

to remove the oxide layer. With such a substrate treatment, MgO thin films were grown at temperatures 400–800 °C under high-vacuum conditions ( $5 \times 10^{-6}$  Torr). The duration of deposition ranged from 5 to 10 h.

Several analysis and characterization techniques were used to investigate the MgO thin films. X-ray diffraction (XRD) and X-ray pole figure analysis were performed to determine the crystallinity of the MgO films. The surface morphology was investigated by scanning electron microscopy (SEM). X-ray photoelectron spectroscopy (XPS) was applied to study the compositions in the MgO films.

**Thermal Desorption Studies.** Experiments were performed in the UHV CVD chamber equipped with a differentially pumped quadrupole mass analyzer (QMA, Balzers QMG511). For temperature-programmed desorption (TPD) and integrated desorption mass spectrometry (IDMS) experiments, the heating rate was 1 °C/s. Dosing of the MMTB precursor was performed with an effusive molecular beam doser. The Si substrates were held about 2 mm from the quadrupole mass analyzer skimmer during TPD and IDMS experiments.

## Results and Discussion

**Synthesis and Characterization of MMTB.** The tetranuclear cubane complex  $[\text{MeMgO}^t\text{Bu}]_4$  was synthesized from methylmagnesium bromide by the precipitation reaction with potassium *tert*-butoxide in a refluxed toluene solution, which has been modified from the method reported by Ashby and co-workers.<sup>31</sup> The product was obtained quantitatively, and crystallized in the form of colorless crystals by cooling a supersaturated solution of MMTB in hexane.

The  $^1\text{H}$  and  $^{13}\text{C}$  NMR spectra of MMTB clearly confirm that the product is a pure tetranuclear cubane complex, by comparison with the reported data.<sup>31</sup> The crystal structure of MMTB was also determined by single-crystal X-ray crystallography.

The molecular structure of MMTB and its atomic numbering scheme are displayed in Figure 1. Atomic positional and thermal parameters, and selected bond distances and angles are summarized in Tables 2 and 3, respectively. The crystal structure consists of a tetrameric cubane of  $[\text{CH}_3\text{Mg}(\mu_3\text{-OC}(\text{CH}_3)_3)_4$  as predicted from the association study by Ashby's group.<sup>31</sup> The central moiety is a cubane  $\text{Mg}_4\text{O}_4$  similar to  $[\text{Mg}(\text{thd})(\mu_3\text{-OMe})(\text{MeOH})_4]$ ,<sup>21</sup>  $[\text{Mg}(\text{OMe})(\mu_3\text{-OMe})(\text{MeOH})_{1,2}]_4$ ,<sup>34</sup> and  $[\text{Mg}(\eta^5\text{-C}_5\text{H}_5)(\mu_3\text{-OEt})_4]$ .<sup>35</sup> The average

**Table 2. Positional and Equivalent Isotropic Thermal Parameters for  $[\text{Mg}_4\text{Me}_4(\text{O}^t\text{Bu})_4]$**

atom	<i>x</i>	<i>y</i>	<i>z</i>	$U_{\text{eq}}$
Mg1	-0.0971(1)	0.66336(8)	0.42898(5)	0.0543(4)
Mg2	0.1663(2)	0.80454(8)	0.47317(5)	0.0596(4)
Mg3	0.1526(2)	0.70823(8)	0.37624(5)	0.0585(4)
Mg4	-0.0519(2)	0.80839(9)	0.38246(6)	0.0644(4)
O1	0.1271(3)	0.6882(1)	0.44527(9)	0.0500(7)
O2	-0.0567(3)	0.7817(1)	0.45162(9)	0.0519(7)
O3	-0.0704(3)	0.6921(2)	0.36179(9)	0.0566(7)
O4	0.1698(3)	0.8230(2)	0.4025(1)	0.0574(7)
C1	0.1952(5)	0.6362(3)	0.4711(2)	0.065(1)
C2	0.1384(6)	0.5545(3)	0.4398(2)	0.101(2)
C3	0.3611(5)	0.6689(3)	0.4772(2)	0.099(2)
C4	0.1541(6)	0.6360(3)	0.5211(2)	0.097(2)
C5	-0.1426(6)	0.8119(3)	0.4825(2)	0.075(1)
C6	-0.3001(6)	0.7857(4)	0.4553(2)	0.115(2)
C7	-0.0822(7)	0.9007(3)	0.4926(3)	0.132(3)
C8	-0.1268(7)	0.7773(4)	0.5295(2)	0.122(2)
C9	-0.1664(5)	0.6446(3)	0.3157(2)	0.083(2)
C10	-0.3222(6)	0.6478(4)	0.3158(2)	0.115(2)
C11	-0.1581(7)	0.5606(4)	0.3142(2)	0.123(2)
C12	-0.1100(7)	0.6804(5)	0.2738(2)	0.136(3)
C13	0.2765(6)	0.8903(3)	0.3912(2)	0.080(2)
C14	0.2556(6)	0.9646(3)	0.4161(2)	0.107(2)
C15	0.2438(7)	0.8835(3)	0.3350(2)	0.115(2)
C16	0.4296(6)	0.8845(3)	0.4101(3)	0.119(2)
C17	-0.2592(5)	0.5722(3)	0.4458(2)	0.095(2)
C18	0.3074(6)	0.8695(4)	0.5390(2)	0.127(2)
C19	0.2825(6)	0.6663(3)	0.3336(2)	0.103(2)
C20	-0.1622(7)	0.8786(4)	0.3462(3)	0.132(3)

**Table 3. Selected Bond Distances of  $[\text{Mg}_4\text{Me}_4(\text{O}^t\text{Bu})_4]$**

Mg1–O1	2.051(3)	Mg1–O2	2.054(3)
Mg1–O3	2.049(3)	Mg2–O1	2.051(3)
Mg2–O2	2.051(3)	Mg2–O4	2.051(3)
Mg3–O1	2.052(3)	Mg3–O3	2.059(3)
Mg3–O4	2.056(3)	Mg4–O2	2.055(3)
Mg4–O3	2.050(3)	Mg4–O4	2.057(3)
Mg1–C <sub>Me</sub>	2.099(5)	Mg2–C <sub>Me</sub>	2.097(5)
Mg3–C <sub>Me</sub>	2.097(5)	Mg4–C <sub>Me</sub>	2.100(5)
O–Mg–O	mean: 85.1	[min: 84.6(1) max: 85.6(1)]	
O–Mg–C	mean: 128.6	[min: 126.6(2) max: 130.2(2)]	
Mg–O–Mg	mean: 94.7	[min: 94.0(1) max: 95.3(1)]	

bond distance of Mg–O is 2.053 (3) Å (2.049–2.059), which is in the range of the values 2.05–2.14 Å found in the complexes above. The average bond angles of O–Mg–O and Mg–O–Mg are 85.1° (84.6–85.6) and 94.68° (93.95–95.54), respectively, that are similar to the undistorted values, 84.5–85.6°, and 93.4–95.1° reported for  $[\text{Mg}(\eta^5\text{-C}_5\text{H}_5)(\mu_3\text{-OEt})_4]$ . The internal angle distortion from ideal  $T_d$  geometry of the cubane core is usually found as expansion along the Mg–Mg vector and contraction along the O–O vector, which results in a smaller angle at Mg and a larger angle at O. However, no significant variation occurs in the internal angles of all three pairs of faces of MMTB, whereas one pair of faces showed severe angle distortion (about 3°) compared with the other two pairs for the above-reported complexes.

**Chemical Beam Deposition of MgO Films.** The MgO films were grown on Si(111) and Si(100) substrates at temperatures of 400–800 °C. From cross-sectional SEM images, typical values of the thickness of the films were 2000–3000 Å for 3 h deposition: ~2000 Å at 400 °C, ~2500 Å at 600 °C, ~3000 Å at 700 °C, and ~2000 Å at 800 °C.

*a. XRD Analysis.* Figures 2 and 3 show the evolution of XRD patterns as the growth temperature is increased

(34) Starikova, Z. A.; Yanovsky, A. I.; Turevskaya, E. P.; Turova, N. Ya. *Polyhedron* **1997**, *16*, 967.

(35) Lehmkühl, H.; Mehler, K.; Benn, R.; Ruffinška, A.; Kruger, C. *Chem. Ber.* **1986**, *119*, 1054.

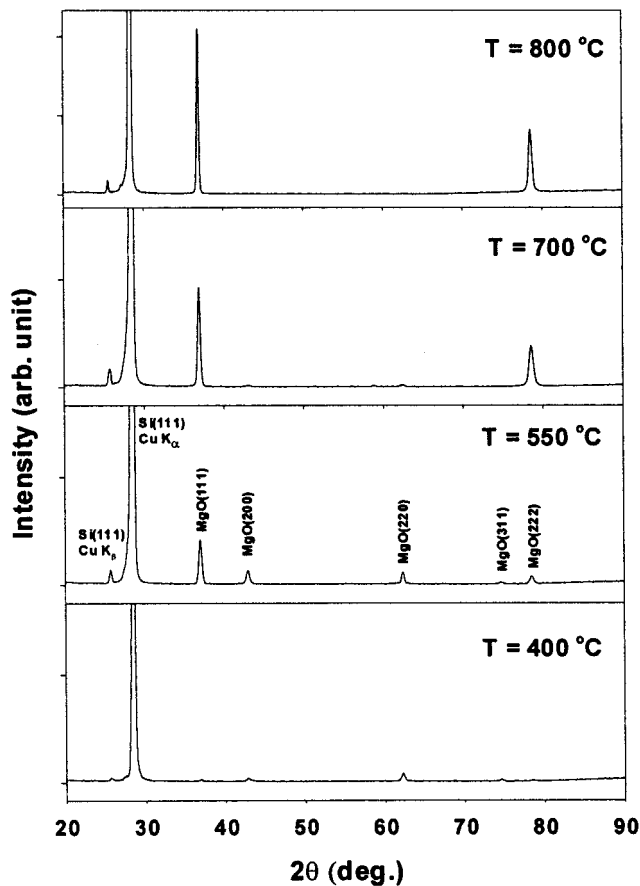


**Figure 2.** XRD patterns of MgO films deposited on Si(111) at varying temperatures.

for the MgO films deposited on Si(111) and Si(100) substrates, respectively. The crystalline structures for the MgO films grown on Si(111) and Si(100) evolved as the growth temperature increased.

XRD patterns for the MgO films grown on Si(111) as a function of deposition temperature are shown in Figure 2. The XRD patterns of the films deposited at 400 °C or lower show either several weak peaks or no peaks, indicating amorphous MgO films were obtained at these temperatures. The XRD pattern of the film deposited at 550 °C clearly displays characteristic peaks of MgO at  $2\theta = 36.9^\circ$ ,  $42.9^\circ$ ,  $62.3^\circ$ ,  $74.7^\circ$ , and  $78.5^\circ$  that are attributed to MgO(111), MgO(200), MgO(220), MgO(311), and MgO(222), respectively. It suggests that a polycrystalline MgO film was obtained at this temperature. At 700 °C, two strong XRD peaks attributed to MgO(111) and MgO(222), but with weak MgO(200) and MgO(220) peaks, appear, indicating predominantly [111] oriented film growth with co-deposition of the [100] and [110] oriented crystallites. Finally, the XRD pattern of the MgO film deposited at 800 °C shows only strong MgO(111) and MgO(222) peaks. This signifies that the MgO film grown at 800 °C possesses a perfect [111] orientation.

A series of XRD patterns for the MgO films grown on Si(100) as a function of deposition temperature is shown in Figure 3. At 400 °C or lower, amorphous or nanocrystalline MgO films were obtained. A polycrystalline MgO film was obtained at 600 °C without any dominant orientation. The XRD pattern of the film deposited at 700 °C indicates a predominantly [100] oriented film

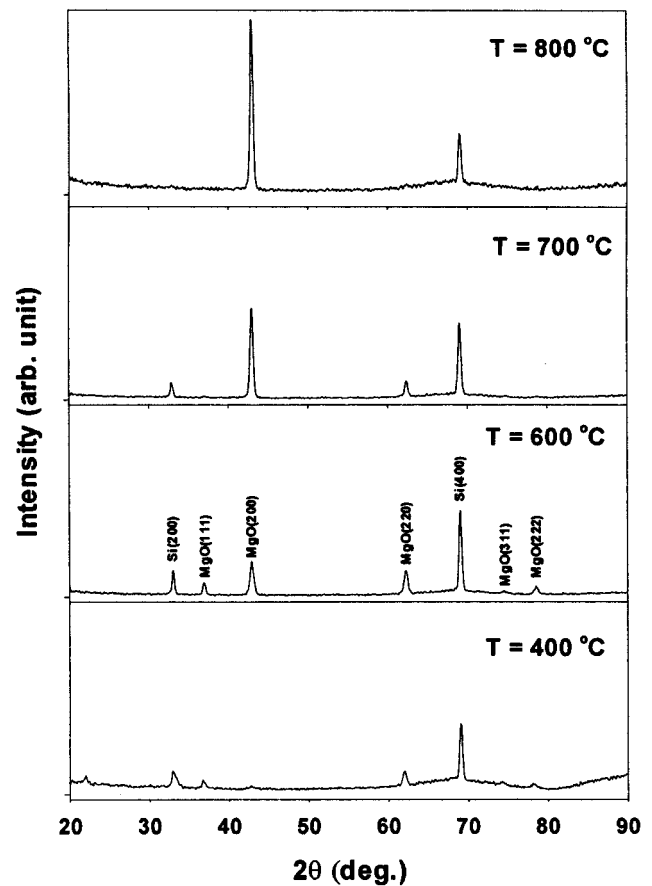


**Figure 3.** XRD patterns of MgO films deposited on Si(100) at varying temperatures.

growth with co-deposition of the [110] oriented crystallites. Finally, a MgO film was grown at 800 °C with the highly preferred orientation toward the [100] direction.

*b. X-ray Pole Figure Analysis.* A pole figure is a stereographic projection, with a specified orientation relative to the sample, which shows the variation of pole density with pole orientation for a selected crystal plane. X-ray pole figure analysis was used to determine whether the MgO film was grown epitaxially. The pole figures of the MgO films deposited on Si(111) and Si(100) substrates at 800 °C are shown in Figure 4. For the MgO film on Si(111), six (100) poles are shown at  $60^\circ$  intervals circularly; the angle from the surface normal is  $54.7^\circ$ , which is the angle between the (111) plane at the center and the (100) plane. This pole figure is similar to the corresponding pole figure (not shown) of a single-crystalline MgO(111) substrate, which clearly demonstrates that the film was epitaxially grown on Si(111). However, the (111) poles for the MgO film on Si(100) are distributed almost uniformly over the pole figure, which indicates that the grains have random orientations.

*c. SEM Analysis.* The morphology of the MgO films was examined by SEM. Evolution of the surface morphology of the films shows grain growth behavior as the growth temperature increases. The SEM images for the MgO films deposited on Si(111) and Si(100) at 800 °C are shown in Figure 5. The surface morphology of the MgO film on Si(111) is smooth and uniform with no signs of granular crystallites or microcracks. The SEM image of the MgO film on Si(100) clearly shows the

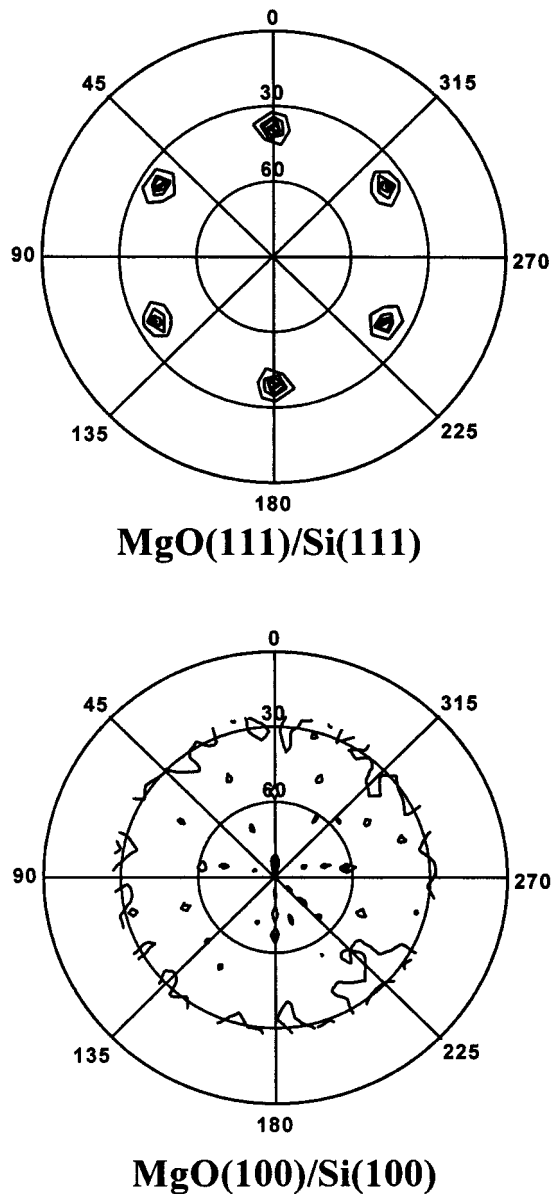


**Figure 4.** Pole figures of MgO films deposited on Si(111) and Si(100) at 800 °C.

square faces of cubic MgO crystallites. However, the surface has a mosaic structure.

*d. XPS Analysis.* XPS analysis was performed to determine the composition of a MgO film deposited on Si(111) at 800 °C. Figure 6 shows the XP spectra of the as-received film and the same film cleaned by Ar<sup>+</sup> ion sputtering. The spectra clearly display the photoelectron and Auger electron peaks for magnesium, oxygen, and carbon only. The ratio of the areas under Mg 1s and O 1s peaks of this film was the same as that of a MgO single crystal. After the surface of the film was sputter etched by an Ar<sup>+</sup> ion beam of 5 keV, the C 1s peak almost disappeared. It indicates that the carbon exists mostly in the surface region of the film. As a result, the XPS analysis evidently shows that the MgO film is stoichiometric and has low levels of impurities.

**Thermal Desorption Studies of MMTB on Si(111) Surfaces.** Thermal desorption studies show that desorption of isobutene and methane occurs between 300 and 498 °C. The identities of desorbing species were determined by integrated desorption mass spectrometry.



MgO(111)/Si(111)



MgO(100)/Si(100)

**Figure 5.** SEM images of MgO films deposited on Si(111) and Si(100) at 800 °C.

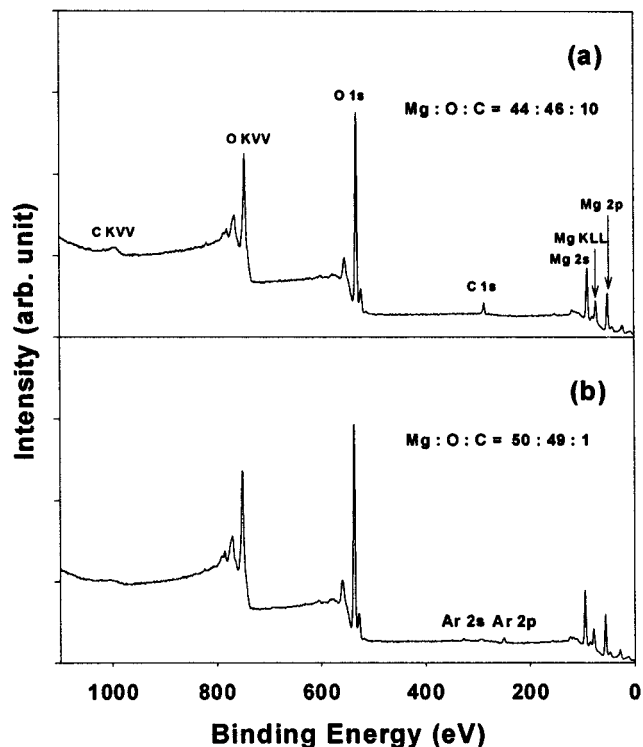


**Figure 6.** XP spectra of an MgO film deposited on Si(111) at 800 °C: (a) as-received; (b) Ar<sup>+</sup> ion sputtered.

Figure 7 (top) shows an IDMS spectrum of the predominant species desorbing from the surface in the 300–500 °C temperature range. Comparison of the top spectrum in Figure 7 to standard mass spectra below indicates that the desorbing species are isobutene and methane. Figure 8 shows temperature-programmed desorption spectra for  $m/e = 41$  and 56 (isobutene) and for  $m/e = 16$  (methane) for MMTB adsorbed on Si(111). Isobutene and methane evolved between 300 and 500 °C ( $T_{\text{max}} = 410$  °C). The prominent signal at  $m/e = 2$  for H<sub>2</sub><sup>+</sup> is mostly due to the H<sub>2</sub> universally present in any UHV system and partly due to cracking of hydrocarbons

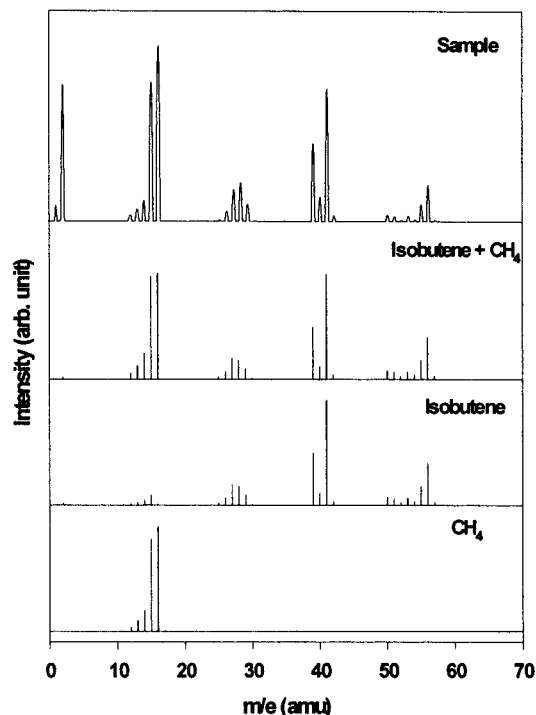


**Figure 7.** Integrated desorption mass spectrum of MMTB (top) with the spectra for isobutene and methane.

at the ionizer of the QMA. The IDMS and TPD results indicate that MMTB decomposes above 297 °C on Si(111) via the  $\beta$ -hydrogen elimination mechanism to yield isobutene and methane in the gas phase, together with adsorbed MgO intermediates. Although the precursor exists as a tetramer in the gas phase, we may envision its pyrolysis process on the substrate surface by using a monomeric form as shown in Scheme 1, which was originally suggested by Ashby et al.<sup>28</sup> The  $\beta$ -hydrogen elimination is the first step in the decomposition sequence of MMTB on Si(111). The next steps in the sequence, which involve the fate of adsorbed MgO intermediates, are not clear at present.

?Author---See paragraph above. Please identify QMA.

### Conclusions

MgO films were grown on Si(111) and Si(100) at 800 °C by metal organic chemical beam deposition under high-vacuum conditions by using methylmagnesium *tert*-butoxide. XRD and X-ray pole figure analysis showed that MgO films with good crystallinity could be epitaxially formed on Si(111) at 800 °C. The MgO films, from XPS analysis, are also stoichiometric and have low

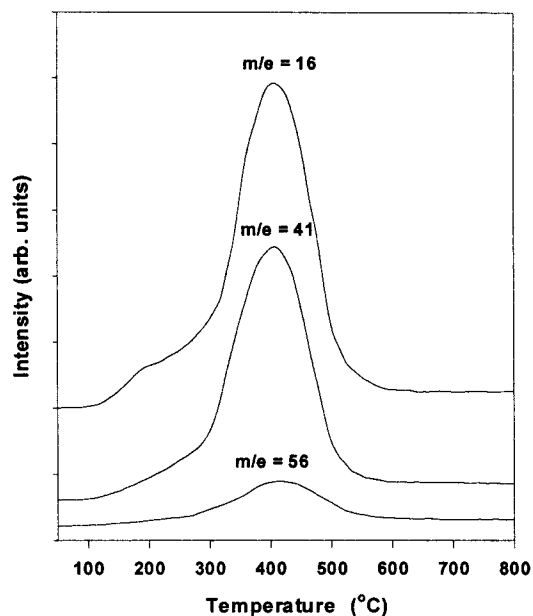
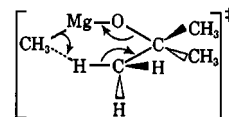


**Figure 8.** Temperature-programmed desorption spectra of MMTB for various species.

### Scheme 1. Proposed Mechanism for the Pyrolysis of Methylmagnesium *tert*-Butoxide



levels of impurities. From these results we have found that the single precursor, methylmagnesium *tert*-butoxide, with a Mg/O ratio of 1:1, is suitable for the epitaxial growth of magnesium oxide on Si(111) substrates. In contrast, highly [100] oriented MgO films with a mosaic structure could be formed on Si(100) at 800 °C.

Thermal desorption studies show that MMTB decomposes above 297 °C on Si(111) via the  $\beta$ -hydrogen elimination mechanism to yield isobutene and methane in the gas phase, together with adsorbed MgO intermediates. In conclusion, the single precursor methylmagnesium *tert*-butoxide has been found suitable for chemical beam deposition of MgO thin films on Si substrates.

**Acknowledgment.** This work was supported by the Ministry of Science and Technology of Korea.

CM010683X